



HAL
open science

Molecular structure of poly methyl methacrylate thermoreversible gels

Nazir Fazel, Zarmina Fazel, Annie Brûlet, Jean-Michel Guenet

► **To cite this version:**

Nazir Fazel, Zarmina Fazel, Annie Brûlet, Jean-Michel Guenet. Molecular structure of poly methyl methacrylate thermoreversible gels. *Journal de Physique II*, 1992, 2 (8), pp.1617-1629. 10.1051/jp2:1992224 . jpa-00247755

HAL Id: jpa-00247755

<https://hal.science/jpa-00247755>

Submitted on 4 Feb 2008

HAL is a multi-disciplinary open access archive for the deposit and dissemination of scientific research documents, whether they are published or not. The documents may come from teaching and research institutions in France or abroad, or from public or private research centers.

L'archive ouverte pluridisciplinaire **HAL**, est destinée au dépôt et à la diffusion de documents scientifiques de niveau recherche, publiés ou non, émanant des établissements d'enseignement et de recherche français ou étrangers, des laboratoires publics ou privés.

Classification

Physics Abstracts

61.12 — 81.20S — 82.70

Molecular structure of poly methyl methacrylate thermoreversible gels

Nazir Fazel (^{1, 2}), Zarmina Fazel (¹), Annie Brûlet (³) and Jean-Michel Guenet (^{1*})

(¹) Laboratoire d'Ultrasons et de Dynamique des Fluides Complexes (**), Université Louis Pasteur-CNRS URA 851, 4 rue Blaise Pascal, F-67070 Strasbourg Cedex, France

(²) Laboratoire de Physique des Liquides et Interfaces, Université de Metz, 57070 Metz Cedex, France

(³) Laboratoire Léon Brillouin (CEA-CNRS), CEN Saclay, F-91191 Gif-sur-Yvette Cedex, France

(Received 17 March 1992, accepted in final form 30 April 1992)

Abstract. — The molecular structure of PMMA gels and aggregates in bromobenzene and *ortho*-xylene has been investigated by small-angle neutron scattering. It is found that in bromobenzene the gels are constituted of connected, prolate cylinder-like structures. A large proportion of these structures (about 90 %) possess a radius of about 1.5 nm. The remaining possess larger radii (from 3.0 to 5.3 nm). On heating, the melting process seems to proceed *via* two-steps : melting of the junction domains while the cylinder-like structures remain virtually unaffected. Scattering curves that differ significantly are obtained in *ortho*-xylene. They are also interpreted with cylinder-like objects of larger radii (up to 10 nm). As with bromobenzene, melting seems to take place in two steps. These results prove to be relevant for interpreting rheological data that will be presented in a forthcoming paper.

Introduction.

The aggregation and/or thermoreversible gelation of stereoregular poly methyl methacrylate has received considerable attention these past 25 years. Many investigations have been carried out with different techniques on *syndiotactic* PMMA (sPMMA) and on the so-called stereocomplex *syndiotactic* PMMA + *isotactic* PMMA (iPMMA). A comprehensive review on the subject has been recently authored by Spevacek and Schneider [1].

Gelation of the syndiotactic PMMA shows some interesting aspects as it is said to proceed in two steps : helix formation followed by helix aggregation [2, 3]. In addition, PMMA is to our knowledge the only synthetic polymer for which the occurrence of double helices in gels and aggregates is reported [4, 5]. As such it may be regarded as the synthetic counterpart of polysaccharides gels [6].

(*) To whom correspondence should be addressed.

(**) Formerly Laboratoire de Spectrométrie et d'Imagerie Ultrasonores.

While much has been gained on the formation conditions (see for instance Refs. [2, 3, 7-11], the short range structure by NMR [12] and the possible helical forms involved [13], no investigations have been carried out so far on the submicronic molecular structure (that is in the range 10-1 nm). This is the aim of this paper to report on experiments achieved by means of neutron scattering on the gels and pregels of this polymer. The molecular structure has been studied as a function of both the solvent type and temperature. The results detailed herein will be of further use for examining, from a molecular viewpoint, the rheological properties of these gels which will be reported in a forthcoming paper [14].

Experimental.

MATERIALS. — Two PMMA samples have been used in this study. They are referred to as PMMA1 and PMMA2. PMMA1 was supplied by Röhm GmbH (Germany) while PMMA2 was purchased from PSS (Mainz, Germany). Their molecular weight and molecular weight distribution have been determined by GPC in THF at 20 °C using columns calibrated with polystyrene standards (universal calibration method). The results are as follows :

$$\begin{aligned} \text{PMMA1 } M_w &= 1.06 \times 10^5 & \text{and } M_w/M_n &\approx 2.86 \\ \text{PMMA2 } M_w &= 7 \times 10^4 & \text{and } M_w/M_n &\approx 1.48 . \end{aligned}$$

Determination of tacticity has been performed in deuterated chloroform by means of $^1\text{H-NMR}$. The following figures were obtained for the isotactic triads (*i*), heterotactic triads (*h*) and the syndiotactic triads (*s*) :

$$\begin{aligned} \text{PMMA1 } i &= 18 \% , h = 15 \% & \text{and } s &= 67 \% \\ \text{PMMA2 } i &= 2 \% , h = 25 \% & \text{and } s &= 73 \% . \end{aligned}$$

Deuterated solvents of high purity grade were used : deuterated bromobenzene and deuterated *ortho*-xylene were purchased from Aldrich. In all cases deuteration was over 99 %.

SAMPLE PREPARATION. — Different polymer concentrations were used in this study. For PMMA/bromobenzene systems : 0.0197 g/cm³, 0.029 g/cm³ and 0.17 g/cm³ (designated in what follows as 2 %, 3 % and 17 %, respectively) ; for *ortho*-xylene : 0.029 g/cm³ and 0.17 g/cm³ (designated as 3 % and 17 %, respectively). Homogeneous solutions are first obtained by heating the polymer + solvent mixture close to the solvent's boiling point. These solutions are then quenched at 0 °C for a minimum of 1 h. For 2 %-solutions no macroscopic gel is formed. 2 %-systems were prepared and kept in hermetically closed tubes whereas 3 % systems were prepared the same way but, before gelation could occur, poured into the measuring cell (amorphous silica rectangular cell with an optical path of 0.5 cm). Once these cells were properly sealed the sample was melted again and quenched to room temperature. The 17 %-gels were moulded in a device described elsewhere [15] so as to produce disc-shaped samples of 1 mm thick and 15 mm diameter. The piece of gel was then placed between disc-shaped amorphous silica plates separated by a 1 mm spacer.

In the case of bromobenzene two sets of samples have been prepared. The first set is obtained from the polymer powder as-received (PMMA1). Prior to preparing the second set the polymer powder is subjected to solvent treatment intended for destroying any structures that might have built up during polymerization. This treatment consists of dissolving the polymer powder in a good solvent (chloroform) and of recovering it by precipitation into methanol followed by subsequent drying. In what follows this PMMA sample will be designated as « treated PMMA1 ».

NEUTRON SCATTERING. — The measurements were carried out at the Laboratoire Léon Brillouin (Saclay, France) on PAXY and PACE small-angle cameras. For both cameras the wavelength distribution is characterized by a width at half-height $\Delta\lambda/\lambda_m \approx 8\%$. The main difference between these two cameras lies in the detection system: for PAXY a two-dimensional counter made up with 64×64 cells is used while for PACE the counter is composed of a series of 32 concentric circles (further details available on request). The wavelength, λ_0 , used was 0.5 nm on PAXY and 0.63 nm on PACE. By varying the sample-detector distance the q -range investigated ($q = 4\pi/\lambda_0 x \sin \theta/2$) was typically:

$$0.1 < q(\text{nm}^{-1}) < 1.3.$$

The counter was normalized by means of the incoherent scattering of hydrogenated *cis*-decalin. The scattering due to the solvent as well as the incoherent scattering of the hydrogenated polymer were allowed for by using blanks containing the deuterated solvent plus a given quantity of 2,4 pentanedione. The latter, whose chemical formula is identical to PMMA's monomeric unit ($\text{C}_5\text{H}_8\text{O}_2$), mimics the polymer incoherent signal. Its amount is calculated so that the number of protons per unit volume be the same in the polymer-solvent system and in the blank. The normalized intensity scattered by the polymer then reads:

$$I_N(q) = \frac{\frac{I_s(q)}{T_s \delta_s} - \frac{I_0(q)}{T_0 \delta_0}}{\frac{I_{\text{dec}}(q)}{T_{\text{dec}} \delta_{\text{dec}}} - \frac{I_{\text{ec}}(q)}{T_{\text{ec}} \delta_{\text{ec}}}} \quad (1)$$

in which $I_s(q)$ is the gel intensity, $I_0(q)$ the blank intensity; $I_{\text{dec}}(q)$ the intensity scattered by a 1 mm-decalin sample and $I_{\text{ec}}(q)$ the scattering by the empty cell; δ and T with the appropriate subscript stand for the thickness and the transmission of the different samples.

The reduced form of the absolute intensity scattered by the polymer chains then reads:

$$I_A(q) = I_N(q)/K = C_p S_p(q) \quad (2)$$

where $S_p(q)$ is the polymer structure factor, C_p the polymer concentration and K the calibration constant K given by:

$$K = \frac{(a_p - y_{\text{PD}} a_D)^2 \times 4 \pi \delta_{\text{dec}} N_A T_{\text{dec}}}{g(\lambda)(1 - T_{\text{dec}}) m_p^2} \quad (3)$$

where a_p and a_D are the scattering amplitudes of PMMA and of the deuterated solvent, m_p the molecular weight of the PMMA monomer unit, y_{PD} the ratio of their molar volumes ($y_{\text{PD}} = v_p/v_D$) and $g(\lambda)$ a correction factor which depends upon the neutron wavelength λ_0 and the camera. In the present case the value of $g(\lambda)$ given in reference [16] for D11 and D17 cameras (located at ILL) has been checked to be valid for PACE and PAXY cameras by means of a secondary standard (atactic polystyrene in decalin). Here, g amounts to $g(\lambda_0 = 0.63) = 1.17 \pm 0.05$ and $g(\lambda_0 = 0.5) = 1.27 \pm 0.05$.

Results and discussion.

Before presenting and discussing the results, the gelation ability of the different PMMA samples must be examined. While PMMA1 gives gels in all the solvents investigated, sample PMMA2 does not. Investigations carried out by Spěvaček and coworkers by means of NMR have shown that PMMA aggregation (or gelation) requires to have syndiotactic sequences

possessing a minimum length [17]. The absence of gelation for PMMA2 is thus expected as the mean syndiotactic sequence length can be estimated to be about 6 monomers. That PMMA1, which is globally less syndiotactic than PMMA2, gels may probably stem from the fact that PMMA1 chains contain besides long syndiotactic sequences some amount of isotactic sequences. Under these conditions, the formation of iPMMMA/sPMMA stereocomplex can occur for which the minimum length (syndio or iso) is usually smaller (further reading on these mechanisms can be found in Ref. [1]). The lack of gelation capability of sample PMMA2 led us to investigate PMMA1 gels and aggregates only.

For all the samples investigated the ratio $S/N = \text{signal/noise}$ (i.e. sample intensity/blank intensity) is fairly high as illustrated in figure 1 and in figure 2 wherein are represented the normalized intensities of the samples and of the blanks once corrected for transmission and thickness for PMMA/bromobenzene systems and PMMA/*ortho*-xylene systems, respectively ($\log I(q)$ vs. q). At $q = 1 \text{ nm}^{-1}$, S/N amounts to $S/N \approx 1.56$ (2 %-PMMA/bromobenzene gel), $S/N \approx 2.37$ (17 %-PMMA/bromobenzene gel), $S/N \approx 1.93$ (2 %-PMMA/*ortho*-xylene) and $S/N \approx 4.64$ (17 %-PMMA/*ortho*-xylene).

As will be seen in what follows, the molecular structure of gels and aggregates in bromobenzene or in xylenes differs quite significantly.

EFFECT OF POLYMER CONCENTRATION.

PMMA/bromobenzene aggregates and gels. — As has been aforementioned, polymer-solvent mixtures with $C_p = 2\%$ do not form a gel while mixtures with $C_p \geq 3\%$ do. In fact the critical gelation concentration C_{gel} is slightly lower than 3% in the present case. Results are reported by means of a Kratkyplot ($q^2 I_N(q)$ vs. q) in figures 3, 4 and 5 for 2%, 3% and 17%

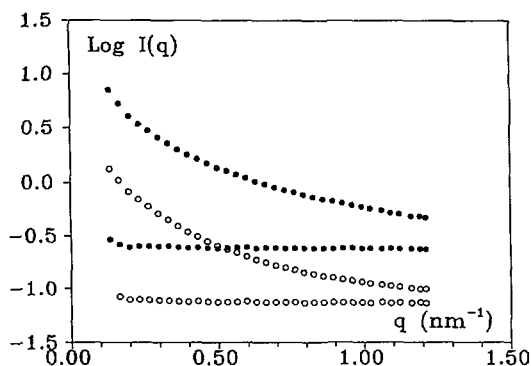


Fig. 1.

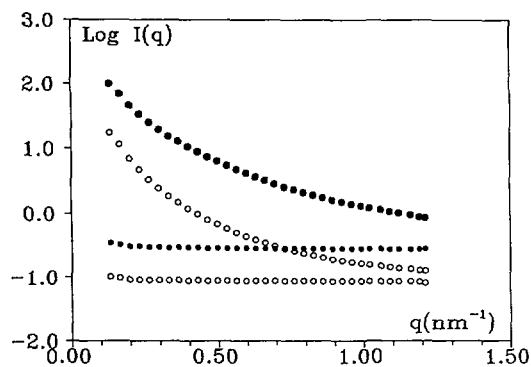


Fig. 2.

Fig. 1. — Intensities (in logarithmic scale) scattered by the PMMA samples (curves with an upturn at small angle) and the corresponding blank (flat curves) once normalized by decalin, thickness and transmission. Solvent = deuterated bromobenzene. (●) 17 %-concentration, (○) 2 %-concentration.

Fig. 2. — Intensities (in logarithmic scale) scattered by the PMMA samples (curves with an upturn at small angle) and the corresponding blank (flat curves) once normalized by decalin, thickness and transmission. Solvent = deuterated *ortho*-xylene. (●) 17 %-concentration, (○) 2 %-concentration.

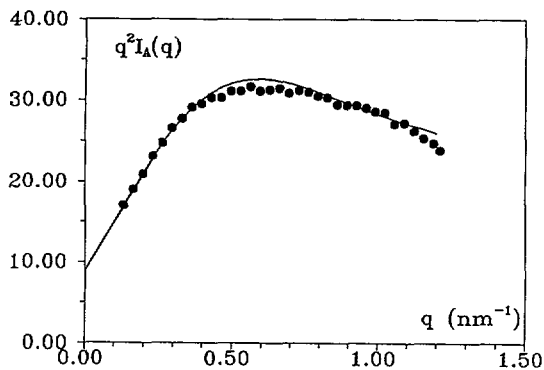


Fig. 3.

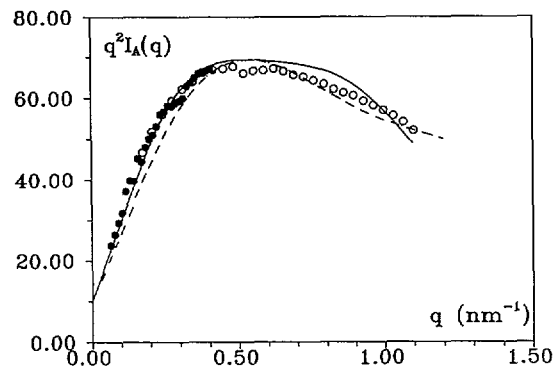


Fig. 4.

Fig. 3. — Kratky-plot, $q^2 I_A(q)$ vs. q , for a 2 %-aggregate in deuterated bromobenzene. The solid line corresponds to a fit obtained with relation (13) (see text for further details).

Fig. 4. — Kratky-plot, $q^2 I_A(q)$ vs. q , for a 3 %-gel in deuterated bromobenzene. The different lines correspond to fits obtained by using relation (13) : dashed line = set 1 ; solid line = set 2 (see text for further details). Filled and open circles correspond to two sample-detector distances.

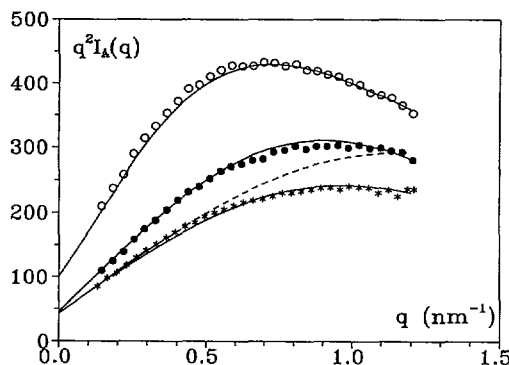


Fig. 5. — Kratky-plot, $q^2 I_A(q)$ vs. q , for 17 %-gels in deuterated bromobenzene. (*) gel prepared with as-received PMMA ; (●) gel prepared with « treated » PMMA ; (○) gel prepared with « treated » PMMA and then swollen to equilibrium in deuterated bromobenzene. The solid lines correspond to fit obtained with relation (10) (for *) and (13) (for ● and ○) (see text for further details). The dashed line corresponds to the scattering by an helix of outer radius 0.9 nm and inner radius 0.7 nm calculated by means of relation (9).

respectively. In all cases the scattered intensity can be fitted with a relation of the type given below :

$$q^2 I_A(q) = C_p [qf(qr) + \text{Cte}] \quad (4)$$

wherein $f(qr) = 1$ for $q = 0$.

The q^{-1} behaviour is well-identified at low q , particularly with the 3 %-gel for which lower q values have been investigated (Fig. 4). Extrapolation to $q = 0$ does not through 0 which

accounts for the constant in equation (4). Finally, departure from the q^{-1} behaviour can be observed at large q -values, hence the function $f(qr)$. This means qualitatively that the molecular structure consists essentially of an *array of rigid rods* possessing a non-negligible cross-section of radius r .

Equation (4) can be rewritten under a more precise form that has been derived by Luzzati and Benoit [18] :

$$q^2 I_A(q) = C_p \mu_L [\pi q \times f(qr) + (-\nu_e + 2.94 \nu_k + 2 \pi^2 \nu_c)] \quad (5)$$

in which μ_L is the mass per unit length (linear mass), ν_e the number of rod ends per unit length, ν_k the number of kinks per unit length and ν_c the number of crossing per unit length with other rods. Presently, the constant term of equation (5) is most probably dominated by ν_c . The function $f(qr)$ can be evaluated in several ways. The rods may consist of either *one helical structure* or an *assembly of helices*. Scattering by infinitely long double helices characterized by a pitch P with cross-section of outer radius r_H , similar to the one portrayed in figure 6, has been derived by Pringle and Schmidt [19] (relation also valid for finite helices of length L and radius r_H provided $qL > 1$ together with $L > r_H$) :

$$I(q) \approx (\pi \mu_L / q) \times \sum_{n=0}^{\infty} \varepsilon_n \cos^2(n\varphi/2) \frac{\sin^2(n\omega/2)}{(n\omega/2)^2} [g_n(qr_H, \gamma)]^2 \quad (6)$$

in which $\varphi = 0$ corresponds to a single helix, n is an integer ($\varepsilon_0 = 1$ and $\varepsilon_n = 2$ for $n \geq 1$) and $(g_n(qr_H, \gamma))$ reads :

$$g_n(qr_H, \gamma) = \frac{2}{r_H^2 (1 - \gamma^2)} \times \int_{\gamma r_H}^{r_H} r J_n[qr \times (1 - a_n^2)^{1/2}] dr \quad (7)$$

in which J_n is the Bessel function of first kind and order n and with the following conditions on the a_n terms :

$$\left. \begin{array}{ll} a_n = 2 \pi n / qP & \text{for } q > 2 \pi n / P \\ a_n = 1 & \text{for } q \leq 2 \pi n / P \end{array} \right\} \quad (8)$$

Here, only the value $n = 0$ has to be considered since $n = 1$ is likely to correspond to $a_1 = 1$. As a matter of fact, $a_1 \neq 1$ requires $P > 5.2$ nm. So far there has been no report

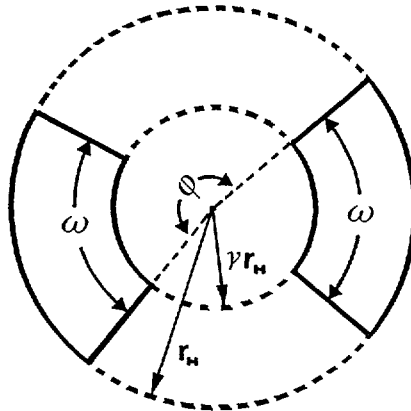


Fig. 6. — Schematic representation of the cross-section of a double helix of outer radius r_H and inner radius γr_H as considered by Pringle and Schmidt for deriving relation (6).

concerning either sPMMA crystals or the stereocomplex helical form of pitches larger than this value [5]. Under these conditions relation (6) reduces to the more simple form independent of whether single helices or double helices are dealt with :

$$I(q) \approx (\pi \mu_L / q) \times \left\{ \frac{2}{(1 - \gamma^2) \times q r_H} \times \{J_1(q r_H) - \gamma J_1(q \gamma r_H)\} \right\}^2 \quad (9)$$

The intensity scattered by an assembly of helices that may be forming a prolate rod-like structure with circular cross-section, reads [20] :

$$I(q) \approx (\pi \mu_L / q) \times \left(\frac{2 J_1(q r)}{q r} \right)^2 \quad (10)$$

which corresponds to relation (9) by equating $\gamma = 0$. $f(qr)$ is then given by the expression between bracket in (9) and (10).

As can be seen in figure 5, relation (10) gives a very good fit to the experimental results by considering a rod-like structure with a circular cross-section $r = 1.4 \pm 0.05$ nm (gel prepared with PMMA as-received and non-swollen). Here, the constant in relation (4) is determined experimentally after extrapolation to $q = 0$ of the linear part of the scattering curve.

Such a value for the radius is larger than the one expected for one double helix of the stereocomplex considering the latest structure determined by Schomaker and Challa [21] ($r_H \approx 1.1$ nm and $\gamma \approx 0$). Alternatively, a fit by means of relation (9) by considering this time the helical form suggested by Kusuyama *et al.* [5] (74 monomer units in four turns, $P = 3.54$ nm $r_H = 0.9$ nm and $\gamma = 0.77$) is not appropriate either (see Fig. 5). A near-trans helix is not suitable either ($r_H < 0.5$ nm, $\gamma \approx 0$).

Yet, it is worth emphasizing that a problem of contrast may arise due to helix solvation [5]. If the molar volume of the solvent incorporated in the helical structure differs from the one in the liquid, then the following relation should rather be considered :

$$I(q) \approx (\pi \mu_L / q) \times \left\{ \frac{2 A_c}{q \gamma r_H} J_1(q \gamma r_H) + \frac{2 A_e}{(1 - \gamma^2) \times q r_H} \times \{J_1(q r_H) - \gamma J_1(q \gamma r_H)\} \right\}^2 \quad (11)$$

in which A_c and A_e are the scattering amplitudes, with respect to the envioning solvent, of the inner part and of the outer part, respectively. As these amplitudes can be of opposite signs apparent cross-section radii can be smaller than the actual one.

Further data can be gained from the $1/q$ part of the scattering curve, i.e. the linear mass of the rod-like structure. For the non-swollen 17 %-gel (as-received PMMA), μ_L amounts to $\mu_L = 680 \pm 60$ g/nm \times mole. The 74₄ helix suggested by Kusuyama *et al.* [5] would give $\mu_L = 2\,090$ g/nm \times mole without taking into account the occluded solvent. A near-trans helix would yield $\mu_L \approx 500$ g/nm \times mole. The double-stranded helix of the stereocomplex should yield $\mu_L \approx 1\,470$ g/nm \times mole [21].

Thus, the combination of the experimental linear mass and radius r cannot be reconciled neither with rods being composed of one helical form as those reported in the literature (r is too low) nor with a simple bunch of helices (value of r alright but value of μ_L too low). (Proton exchange between the polymer and the solvent, that would have produced the same effect on μ_L , has been discarded on the basis of proton NMR testing). This may suggest that the rod-like structures consist of a *bunch of solvated helices*. The present data do not enable one to draw further conclusions as to the nature of the helices. Whether the rods may consist of a mixture of double helices due to stereocomplex formation or of single helices due to sPMMA self-association is not important for the present analysis.

Alternative models, that can account for the low linear mass, are also worth envisaging : i) a network of rod-like structure in which independent Gaussian chains of radius R are embedded (alternative 1) or ii) a network of alternating rod-like, ordered sequences with Gaussian-like, disordered sequences of end-to-end distance $\langle s^2 \rangle^{1/2}$ (alternative 2). In both cases the Gaussian entity may give a q^{-2} behaviour (provided $qR > 5$ or $q \langle s^2 \rangle^{1/2} > 9$), hence contributing to the value of the constant in relation (4) and (5).

In both cases if $1 - X$ is the amount of disordered Gaussian material then the following relation must be used instead of (4) :

$$q^2 I_A(q) = C_p \mu_L [Xqf(qr) + \text{Cte}] . \quad (12)$$

As X is lower than 1 the use of relation (5) instead of relation (12) is to entail an underestimate of μ_L . For μ_L to reach a value high enough, such as $1470 \text{ g/nm} \times \text{mole}$, X should be about 0.45. This represents a high content of disordered material ($1 - X = 0.55$) a figure which is not strictly born out by results gained on the other concentrations nor by the rheological properties reported in a forthcoming paper [14]. While the very presence of disordered material cannot be discarded, its amount is likely to be lower than 55 %.

To summarize, the gel consists most probably of interconnected rods that consist themselves of aggregated, solvated helices.

The gel prepared with the « treated » PMMA1 gives a scattering curve noticeably different from the previous one which cannot be accounted for by experimental uncertainties (this effect is also seen on the mechanical properties as shown in the forthcoming paper [14]). Here again the fit can be achieved with relation (10) and one radius, i.e. $r = 1.5 \pm 0.05 \text{ nm}$. The linear mass is found to be $\mu_L = 870 \pm 90 \text{ g/nm} \times \text{mole}$ (Fig. 5).

Whereas results gained on non-swollen gels can be fitted with one single radius, this is no longer the case for the *swollen gel* (after swelling the concentration is $C_p = 0.0924 \text{ g/cm}^3$). Provided the cross-section radius be always smaller than the distance between crossing zones, $I(q)$ can be regarded as the superposition of the intensity scattered by those rod-like structures of radius r_i and concentration C_i .

$$q^2 I_A(q) = \sum_i q^2 I_{A_i}(q) = \sum_i C_i q^2 S_i(q) = C_p \left(\sum_i \pi q w_i \mu_{L_i} \frac{4 J_1^2(qr_i)}{(qr_i)^2} + \text{Cte} \right) . \quad (13)$$

The scattering curve can be fitted by considering the simplest distribution, i.e. two different values for r_i . Bearing in mind that $\mu_{L_i} \approx r_i^2$ for a circular cross-section, a good fit can be obtained with the following values (Fig. 5) :

$$\begin{aligned} r_1 &= 1.5 \text{ nm} & w_1 &= 0.88 \\ r_2 &= 3.0 \text{ nm} & w_2 &= 0.12 . \end{aligned}$$

The experimental linear mass amounts now to $\langle \mu_L \rangle_w = 1250 \text{ g/nm} \times \text{mole}$.

The occurrence of rod-like segments with larger cross-sectional radius may originate in the « crystallization » of independent, free chains entrapped in the network that have been already considered above. The swelling of the network probably enhances their mobility and correspondingly their capability of ordering onto the existing rod-like segments. This mechanism may proceed *via* deposition of syndiotactic material onto the already-ordered syndiotactic rods but also *via* the formation of stereocomplex.

The results obtained with the 3 %-gels can also be simply fitted with two radii, although we have found out that at least two sets of value can be considered (see Fig. 4) :

$$\left. \begin{array}{ll} r_1 = 1.5 \text{ nm} & w_1 = 0.8 \\ r_2 = 3.5 \text{ nm} & w_2 = 0.2 \end{array} \right\} \text{ set 1}$$

$$\left. \begin{array}{ll} r_1 = 2.0 \text{ nm} & w_1 = 0.91 \\ r_2 = 5.3 \text{ nm} & w_2 = 0.09 \end{array} \right\} \text{ set 2 .}$$

Here, the linear mass is $\mu_L \approx 2\,280 \text{ g/mole} \times \text{nm}$. If one considers that rods density is independent of rod diameter then one can estimate the linear mass for set 1 and set 2 by using the results obtained from the non-swollen « treated » PMMA1 ($870 \text{ g/mole} \times \text{nm}$ for $r = 1.5 \text{ nm}$). Under these conditions the value of $\mu_L = 2\,380 \text{ g/mole} \times \text{nm}$ calculated for set 2 is in better agreement with the experimental value. At any rate these fits do indicate that the 3 %-gel is, as the swollen 17 %-gel, constituted of a large proportion of rods of cross-section radius of about 1.5 nm to 2.0 nm and a small yet non-negligible proportion of rods with a larger cross-section radius. It is worth mentioning that we did not succeed in fitting the experimental curves when using continuous distributions such as slot function distribution ($w_i = \text{Cte}$) or Gaussian distribution.

That the 3 %-gel resembles the *swollen* 17 %-gel is not surprising. Being so close to the critical gelation concentration, it is virtually produced under equilibrium swelling conditions.

In the case of the 2 %-system, which produces aggregates but no three-dimensional network, the theoretical fits yield essentially the same results (Fig. 3) :

$$\begin{array}{ll} r_1 = 1.5 \text{ nm} & w_1 = 0.84 \\ r_2 = 3.4 \text{ nm} & w_2 = 0.16 \end{array}$$

with $\mu_L = 1\,000 \text{ g/mole} \times \text{nm}$ a value lower than what is theoretically expected ($1\,400 \text{ g/mole} \times \text{nm}$) from the assumptions discussed above.

These 2 %-aggregates are certainly branched as the constant of relation (4) differs from 0. *PMMA/ortho-xylene gels*. — Here are discussed the results obtained on a 17 %-gel. Those obtained on the 3 %-gels will be postponed to the section devoted to temperature effects.

The results are drawn in figure 7 by means of a Kratky-plot. As is apparent from this figure, the behaviour differs significantly from the one observed in bromobenzene. In particular, no maximum is seen. Presently, we can think of two ways of tackling the problem : either by considering this particular scattering pattern to arise from the fractal dimension of the connecting objects (approach 1) or by regarding the gel to be made up with rod-like connecting objects possessing larger cross-section radii (approach 2).

A log-log plot of the scattered intensity yields a terminal slope of 2.7 ± 0.05 (see Fig. 8). Since the domain of distance under consideration in this q -range lies between 3 nm to about 0.9 nm, then this slope may be taken for the purpose as the fractal dimension, ν^{-1} , of the objects connecting the junction domains should approach 1 be valid. Yet, as will be seen in the forthcoming paper [14], the variation of the gel modulus as a function of polymer concentration is not consistent with this approach. Also, this would imply objects with negligible cross-section, an assumption difficult to reconcile with other data.

In our opinion, it seems more judicious to regard the gel molecular structure being similar to the one in bromobenzene and to contemplate the possible presence of rod-like connecting objects possessing larger cross-section (approach 2). As above, the use of continuous distribution proved to be to no avail. A reasonable fit has been obtained by considering a set of three values with the following weight fractions (see Fig. 7) :

$$\begin{array}{ll} r_1 = 1.5 \text{ nm} & w_1 = 0.7 \\ r_2 = 4.0 \text{ nm} & w_2 = 0.2 \\ r_3 = 10.0 \text{ nm} & w_3 = 0.1 . \end{array}$$

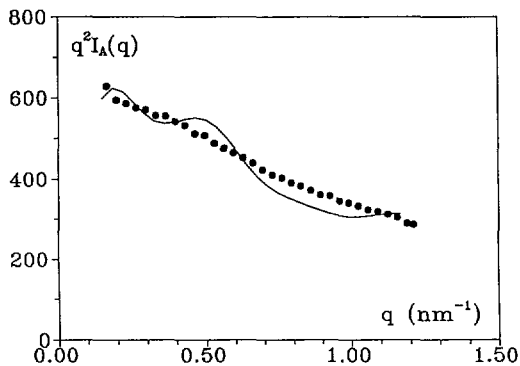


Fig. 7.

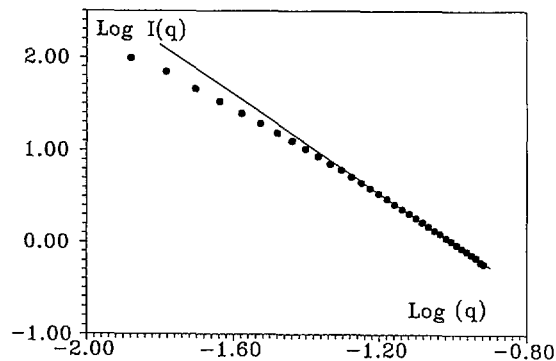


Fig. 8.

Fig. 7. — Kratky-plot, $q^2 I_A(q)$ vs. q , for a 17 %-gel in *ortho*-xylene. The solid line corresponds to a fit obtained from relation (13) (see text for further details).

Fig. 8. — Log-log plot of the intensity scattered by a 17 %-gel. The solid line corresponds to a slope of 2.67.

Evidently, this fit is not as good as those given for PMMA/bromobenzene gels or aggregates and, therefore, must be simply regarded as indicative. Improvement could possibly be achieved by entering 4 or 5 radius values instead of only three in relation (13). This fit essentially indicates that a discrete distribution rather than a continuous one seems more appropriate. Provided approach 2 be correct, then it appears that the growth of thicker fibrils is favoured in *ortho*-xylene with respect to bromobenzene. This phenomenon may not be surprising since *ortho*-xylene appears to be a solvent poorer than bromobenzene. It is worth noticing that this approach hints at the presence of a large amount of objects with a cross-section of 1.5 nm as in bromobenzene. This may suggest the existence of some basic structure. However, we have so far considered the connecting objects to be rod-like, that is possessing a fractal dimension $\nu^{-1} = 1$. Rheological behaviour invite to suggestion that their fractal dimension might be higher than 1 in which case relation (4) should rather read :

$$q^2 I_A(q) = C_p [q^{2-\nu} f(qr) + o(q^{2-2\nu})]. \quad (14)$$

This will obviously modify the values of r in $f(qr)$. Clearly, further investigations are now much needed to elucidate the molecular structure of PMMA gels in *ortho*-xylene.

EFFECT OF TEMPERATURE.

PMMA/bromobenzene gels. — The alteration of molecular structure on a 3 %-gel prepared at 0 °C has been examined at three different temperatures above room temperature, namely 45 °C, 70 °C and 90 °C. It is worth stressing that at 90 °C the gel is not macroscopically molten. As can be seen in figure 9 the shape of the curves remain essentially the same while a global shift toward lower intensity values seems to occur. This would mean that only the constant term in relation 4 is modified. This statement is better illustrated when subtraction is made of the constant term determined for each temperature at $q = 0$ as all the scattering curves are now virtually superimposable (Fig. 10).

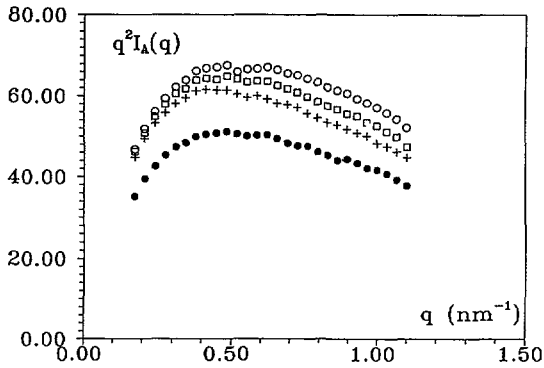


Fig. 9.

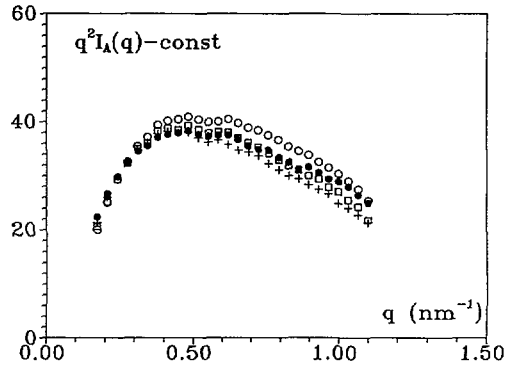


Fig. 10.

Fig. 9. — Kratky-plot, $q^2 I_A(q)$ vs. q , for a 3 %-gel in bromobenzene prepared at 0 °C and then heated at different temperatures : (O) 20 °C, (□) 45 °C, (+) 70 °C, (●) 90 °C.

Fig. 10. — Same results as in figure 9 (3 %-gel in bromobenzene) except that a constant term has been subtracted (see text for further details) : (O) 20 °C, (□) 45 °C, (+) 70 °C, (●) 90 °C.

This result hints at a possible two-step melting process : schematically, the first step would involve the melting of the junctions while the second step would involve the very melting of the rod-like objects. This would then be most reminiscent of the two-step mechanism put forward by Sedlacek *et al.* [2] and, later, by Berghmans *et al.* [3] for the formation process. In this case these authors report that helical structures build first and then aggregate. The reverse situation is likely to occur on melting.

PMMA/ortho-xylene gels. — Results obtained on 3 %-PMMA/*ortho*-xylene gels are reported in figure 11 for different temperatures. One can distinguish two sets of curves : at 20 °C and 30 °C no change can be detected whereas at $T = 54.5$ °C a significant loss of intensity at the smallest scattering vectors has occurred. Above 54.5 °C the modification of the scattering patterns are but minor. Besides, the scattering patterns merge at the largest scattering vectors. Interpretation of these results is not straightforward and poses the same questions as

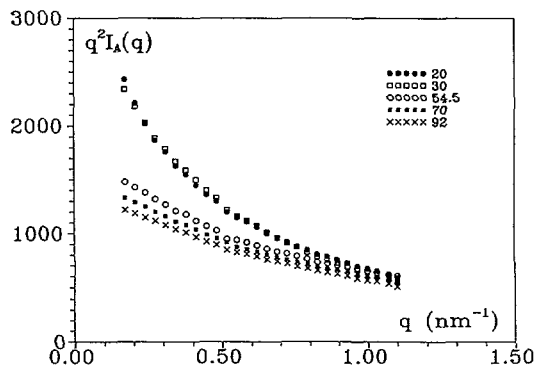


Fig. 11. — Kratky-plot, $q^2 I_A(q)$ vs. q , for a 3 %-gel in *ortho*-xylene prepared at 0 °C and then heated at different temperatures : (●) 20 °C, (□) 30 °C, (○) 54.5 °C, (■) 70 °C, (×) 92 °C.

those evoked with the 17 %-gel. The strong decrease of the forward scattering at higher temperatures may suggest the disappearance of rod-like objects with very large cross-sections, which would be, incidentally, far larger than in the 17 %-gels.

The effect of sample's inhomogeneity may also be contemplated in those 3 %-gel that formed just above the critical gel concentration. Under these conditions, that gel porosity be inhomogeneous, as portrayed in figure 12, would not be totally unexpected. Then one may expect, on top of the rod-scattering, an excess scattering such as described by Debye-Bueche [22] :

$$I_{\text{ex}}(q) = (1 + q^2 a^2)^{-2} \quad (15)$$

in which a represents a correlation length between the different domains.

If, on melting, inhomogeneities vanish and provided the basic gel structure be the same, then a pattern much similar to the one obtained with the 17 %-gel should be observed as the excess term $I_{\text{ex}}(q)$ should fade out. This is what is actually seen. The disappearance of inhomogeneities may arise from the partial melting of the junctions located in the « highly cross-linked » domains. Further, excess scattered intensity of the type described by relation (15) rather than the presence of rods with larger cross-sections would better account for the merging at higher q -values of all the scattering curves as I_{ex} should eventually become negligible in this range. If this interpretation is relevant, then PMMA/*ortho*-xylene gel melting would also proceed in two steps in the same way as PMMA/bromobenzene gels.

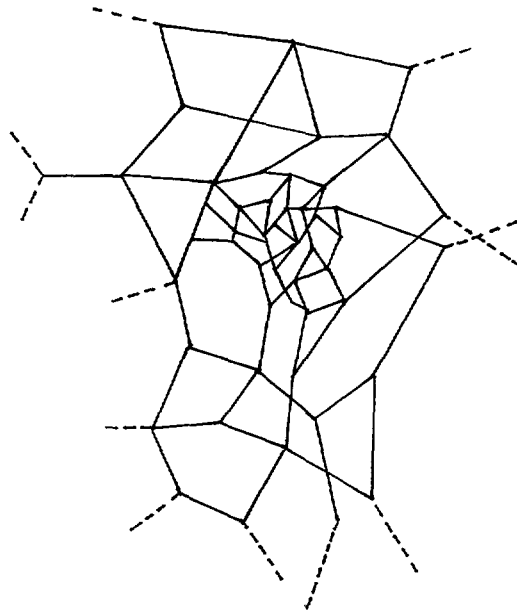


Fig. 12. — Schematic representation of a inhomogeneous gel displaying domains with different mesh size (or porosity).

Concluding remarks.

Physical gels are very often networks of interacting fibrils, the latter usually possessing large diameter in the case of synthetic polymer gels. PMMA gels stand out and resemble closely polysaccharides gels which are constituted of thin threads rather than fibrils. The diameter of

these threads is about the same in PMMA gels, agarose gels [23, 24] and κ -carrageenan gels [25]. Also, in these biopolymer gels two cross-section radii are often considered [23, 26]. While the origin of this similarity remains yet to be understood, PMMA gels may allow one to bridge the apparent gap between thermoreversible polymer gels and biopolymers gels.

References

- [1] SPĚVÁČEK J. and SCHNEIDER B., *Adv. Coll. Int. Sci.* **27** (1987) 81.
- [2] SLEDÁČEK B., SPĚVÁČEK J., MRKVIČKOVÁ L., STEJSKAL J., HORSKA J., BALDRIAN J. and QUADRAT O., *Macromolecules* **17** (1984) 825.
- [3] BERGHMANS H., DONKERS A., FRENAY L., DE SCHRYVER F. E., MOLDENAERS P. and MEWIS J., *Polymer* **28** (1987) 97.
- [4] DYBAL J. and SPĚVÁČEK J., *Makromol. Chem.* **189** (1988) 2099.
- [5] KUSUYAMA H., TAKASE M., HIGASHIHATA Y., TSENG H. T., CHATANI Y. and TADOKORO H., *Polymer Commun.* **23** (1982) 1256.
- [6] ANDERSON N. S., CAMPBELL J. W., HARDING M. M., REES D. A. and SAMUEL J. W. B., *J. Mol. Biol.* **45** (1969) 85.
- [7] BORCHARD W., PYRLIK M. and REHAGE G., *Makromol. Chem.* **145** (1971) 169.
- [8] KÖNNECKE K. and REHAGE G., *Makromol. Chem.* **184** (1983) 2679.
- [9] SPĚVÁČEK J. and SCHNEIDER B., *Coll. Polym. Sci.* **258** (1980) 621.
- [10] SCHOMAKER E., VOREMKAMP E. J. and CHALLA G., *Polymer* **27** (1986) 256.
- [11] SPĚVÁČEK J., SCHNEIDER B., BOHDANECKY M. and SIKORA A., *J. Polym. Sci. Polym. Phys. Ed.* **20** (1982) 1623.
- [12] SPĚVÁČEK J. and SCHNEIDER B., *Polym. Bull.* (1980) 227.
- [13] SPĚVÁČEK J., SCHNEIDER B. and STRAKA J., *Macromolecules* **23** (1990) 3042.
- [14] FAZEL Z., FAZEL N. and GUENET J. M., to be published in *J. Phys. II France*.
- [15] GUENET J. M., *Macromolecules* **20** (1987) 2874.
- [16] RAGNETTI D. and OBERTHÜR R., *Colloid Polym. Sci.* **264** (1986) 32.
- [17] DYBAL J., SPĚVÁČEK J. and SCHNEIDER B., *J. Polym. Sci. Polym. Phys. Ed.* **24** (1986) 657.
- [18] LUZZATI V. and BENOIT H., *Acta Cryst.* **14** (1961) 297.
- [19] PRINGLE O. A. and SCHMIDT P. W., *J. Appl. Cryst.* **4** (1971) 290.
- [20] POROD G., *Acta Phys. Aust.* **2** (1948) 255.
- [21] SCHOMAKER E. and CHALLA G., *Macromolecules* **22** (1989) 3337.
- [22] DEBYE P. and BUECHE A. M., *J. Appl. Phys.* **20** (1949) 518.
- [23] DJABOUROV M., CLARK A. H., ROWLANDS D. W. and ROSS-MURPHY S. B., *Macromolecules* **22** (1989) 180.
- [24] DORMOY Y. and CANDAU D. S. J., *Biopolymers* **31** (1991) 109.
- [25] SUGIYAMA J., TURQUOIS T., TARAVEL F., ROCHAS C. and CHANZY H., submitted.
- [26] HERMANSSON A. M., *Carbohydr. Polym.* **10** (1989) 163.